Low-pressure plasma treatment of CFRP substrates for epoxy-adhesive bonding: an investigation of the effect of various process gases

M. Pizzorni [1,2] · E. Lertora [1] · C. Gambaro [1] · C. Mandolfino [1] · M. Salerno [2] · M. Prato [2]

Abstract
This work reports a systematic and quantitative evaluation of the effects induced on the adhesive properties of carbon fiber reinforced polymer (CFRP) substrates by various vacuum cold-plasma treatments. In particular, surface activation of the CFRP substrates was performed using several combinations of exposure time, plasma power, and processing gas (air, O_2, Ar and N_2). By comparing these plasma treatments with conventional techniques of abrasion and peel ply, it was possible to substantially increase the performance of the adhesively bonded joints made by overlapping the CFRP substrates with a structural epoxy resin. On each differently treated surface, measurements of roughness and of wettability were performed, allowing the evaluation of the increase in surface energy after the plasma treatment. XPS analyses allowed the identification of the chemical state of the substrates and showed an in-depth functionalization of the outer layer of the CFRP material. The experimental results show that an engineered plasma treatment of the CFRP substrates allows one to modify the surface morphology and both wetting and chemical activation properties of the treated surfaces, resulting in an increased mechanical shear strength of the joints.

Keywords Surface treatment · Low-pressure plasma · Carbon fiber reinforced polymer · Epoxy adhesive · Bonding mechanism analysis

Nomenclature

CFRP	Carbon fiber reinforced polymer
LPP	Low-pressure plasma
RT	Room temperature
RF	Radio frequency
SLJ	Single-lap joint
TSS	Tensile shear strength
τ	Average shear strength
S_q	Root mean square height
SFE	Surface free energy
γ_{SV}	Surface energy at the solid-vapor interface
γ_{SV}^p	Polar fraction of γ_{SV}
γ_{SV}^d	Dispersive fraction of γ_{SV}
γ_{SL}	Surface energy at the solid-liquid interface
γ_{LV}	Surface tension at the liquid-vapor interface
γ_{LV}^p	Polar fraction of γ_{LV}
γ_{LV}^d	Dispersive fraction of γ_{LV}
θ	Average contact angle
θ_{H_2O}	Contact angle measured with water droplets
$\theta_{CH_2I_2}$	Contact angle measured with diiodomethane droplets
XPS	X-ray photoelectron spectroscopy
UHV	Ultra-high vacuum
f_P	Pearson's correlation factor

✉ M. Pizzorni
marco.pizzorni@dime.unige.it

[1] Department of Mechanical Engineering, Polytechnic School, University of Genoa, Via All'Opera Pia 15, 16145 Genoa, Italy

[2] Materials Characterization Facility, Istituto Italiano di Tecnologia, Via Morego 30, 16163 Genoa, Italy

1 Introduction

The exponential diffusion of carbon fiber reinforced polymer (CFRP) materials in automotive and aerospace manufacturing [1–3] has led to a widespread and progressive research for techniques that allow the creation of quality joints, at the same time minimizing deterioration of the substrate and damage to the fibers [4]. Therefore, adhesive bonding is now recognized as the best and least invasive method for obtaining joints that ensure high mechanical strength and guarantee excellent quality over time and under different environmental conditions. Indeed, adhesive bonding of plastic composites offers

advantages over riveted structures, overmolding via mechanical interlocking, or other mechanical joining techniques, because the adhesive layer yields a continuous bond between the two substrates, minimizes residual stresses, and acts as a mechanical buffer between the adherends to absorb energy during impact. However, it is well known that obtaining the proper and desired characteristics is not easy and straightforward. Indeed, adhesive bonding requires an engineering of the entire processing, which should involve geometric considerations about areas to be joined, the choice of the most appropriate adhesive according to the conditions under which the component will operate, and proper treatment of the surfaces to be joined. In fact, each adherend-adhesive system has specific properties that are strongly dependent on the characteristics of the substrate. For this reason, it is a common practice to carry out pre-bonding operations aimed at increasing the surface wettability and/or roughness of the surfaces to be joined.

One of the most common surface preparation techniques of CFRP is the peel ply, due to its great ease [5]. However, its use is not always justified, especially when a high and long-lasting performance of the component is required [6]. Mechanical abrasion is also a widely employed treatment, which—thanks to its effect on increasing surface roughness—enhances the resin capability to get into contact with the substrate on which it is applied. However, although widely adopted, even this method presents limitations: firstly, the variability of resulting surface conditions connected to a different experience of the operator makes it difficult to reach the suitable process repeatability; secondly, the mechanical-only action, even if correctly applied, is not always sufficient to fulfill the quality criteria required for the joint [7]. In fact, the bonding process requires a holistic approach, since the premise for good adhesion of resin to substrate lies mainly in the chemical-physical affinity established between the parts involved [8–10]. In the specific case of CFRP substrates, this translates into the need for treatment to fulfill the following objectives:

- to increase the wettability of the CFRP substrate, i.e., to enhance its surface energy so that the adhesive is able to spread easily on substrate independently on its viscosity, without leaving voids and filling any micro-cavities that may be present;
- to activate the surface, increasing functional groups already present or creating new ones, so that they can interact with the adhesive molecules by creating strong covalent bonds with them;
- not to damage the substrate surface, removing too much resin from its matrix until the fibers are uncovered or ruining the reinforcement fibers.

In view of these considerations, modification of CFRP substrates through plasma treatment has recently attracted much attention. In fact, use of plasma on carbon fibers as adhesion promoter to the polymer matrix is already well known [11–13]; in a similar way, also the matrix can be activated following exposure to plasma, both at atmospheric pressure or in vacuum conditions [14–17]. The latter case seems to be preferred for complete preservation of the polymer matrix of CFRP substrates, which do not undergo any heating during the treatment, avoiding the even slight deterioration of the polymer. Thus, low-temperature plasma treatment is promising for pre-bonding activation thanks to its ability to modify the substrate surface without affecting the bulk properties. In addition, the process is highly reproducible since plasma affects the entire component to be treated even in case of complex surface geometry of the specimen.

In other terms, a physical treatment of low-pressure plasma (LPP) may represent for CFRP what chemical etching treatment already represents for metal alloys based on aluminum or titanium [9, 18], entailing increase of both strength and durability of the joints. However, LPP does not suffer the same disadvantages. In fact, although not always cheaper than other treatments, plasma preparation is of course more automatable. In this regard, consider a comparison with chemical treatments typically used on Ti-6Al-4V, such as SHA or NaTESi processes [9, 19, 20]. These envisage a series of critical steps, which contemplate use of hazardous materials and, thus, highly qualified personnel. Thinking about an industrial implementation, this raises the need to provide adequate safety equipment and waste disposal systems, satisfying all strict requirements of the regulations (as an example, DIN 6701 in rail industry). The chemical process must also be constantly monitored, programming periodic and close sampling of the chemical baths aimed at qualifying the maintenance of the solution integrity, as well as the control of all electric parameters, where anodization is performed. Obviously, moreover entailing considerable operating costs, the automatization is certainly reduced compared to a plasma treatment. The latter, indeed, does not require any special preparation of personnel: the operator introduces the material to be treated into the chamber and starts the process according to a pre-defined procedure, setting only parameters such as treatment time and power. The costs referred to in this case are related to the initial investment of the machine (obviously connected to the dimensions of the chamber and the vacuum pumping system) and to the procurement of the process gas. However, as any other surface treatment (chemical, but also physical or mechanical), the need for extensive substrate preparation increases the overall cost of the process and is generally time-consuming, especially when the best treatment conditions are unknown.

In this work, a less conventional technique, vacuum cold-plasma, is compared with the two traditionally most used techniques for pre-treatment of surfaces to be bonded, namely mechanical abrasion and peel ply. An extensive trial campaign

was carried out in order to evaluate the mechanical behavior of the adhesive CFRP joints, plasma-treated with four different gases and several plasma power and exposure-time conditions. Mechanical tests pointed out an increase in joint performance after this treatment and allowed us to select those parameter combinations which provide the best results. It was found that vacuum plasma treatment of CFRP results in a modification of surface morphology as well as in an enhancement of the polar component of surface energy, which reflect the chemical functionalization of the surface involved during this treatment.

2 Experimental

2.1 Materials

The CFRP material used was manufactured with hand lay-up method, arranging five layers of 5H-T800-258gsm carbon plies, pre-impregnated with epoxy resin, with a 0° orientation. Consolidation and curing processes were performed using a vacuum bag in an autoclave for 2 h at 135 °C and pressure of 6 bar. The thickness of the specimens used was 1.55 mm.

A commercial epoxy adhesive, DP490 produced by 3M™, was used to assemble the joints. This is a two-component thixotropic epoxy adhesive designed to be used in applications requiring toughness and high mechanical strength, and thus suitable for making composite joints. This product displays excellent thermal and environmental resistance and has a 90-min work-life, a handling time of 4 ÷ 6 h, and a complete curing time of 7 days (at RT). It was prepared by mixing two parts of epoxy resin and one part of amine-modified curing agent. All joints were tested after 7 days of adhesive bonding, so we did not introduce the variability due to different grades of polymerization.

2.2 Surface preparation and control treatments

Before each treatment—except when peel ply was used—all the substrates were preliminarily wiped with acetone to remove any trace of surface contaminant. Table 1 shows all the treatments performed on CFRP substrates, whose results will be reported in the dedicated section. Two sets of control samples, whose bond area was prepared with conventional techniques such as abrasion and peel-ply removal respectively, were used as references for the mechanical comparison. The abrasion was manually carried out by the same expert operator using a 3M™ Scotch-Brite™ MX-SR abrasive, by superimposing linear movements on directions spaced 45° apart. After abrasion, the surfaces were wiped again with a cotton cloth soaked in acetone, in order to remove all debris of both removed CFRP and abrasive material.

For the samples with the peel ply, any further cleaning procedure is normally required after its removal. This release ply consists in a layer of polyester fabric inserted between mold and consolidation step. Thus, the joints made with this technique were bonded immediately after the removal of the protective ply.

2.3 Plasma treatment

For the surfaces of CFRP laminates treated with LPP, a Tucano multipurpose plasma device (Gambetti Vacuum Technology, Italy) was used. This reactor, schematized in Fig. 1, is powered by an RF generator that operates at a fixed frequency of 13.56 MHz, with maximum power of 200 W. It is equipped with two mass flow controllers (MFC) that allow regulation of a certain percentage of gas flow introduced into the vessel, making it possible to use both a single gas and mixtures of two gases.

The chamber containing the sample to be treated was evacuated to a vacuum level of 0.1 mbar. At this base pressure, the RF power supply was switched on to ignite the plasma discharge between the two electrodes.

In this investigation, four types of gas, namely air, oxygen, argon, and nitrogen, were used, varying both exposure time and plasma power among the values listed in Table 1, for a total of 36 conditions to be considered. It should be noted that other time settings of 5 and 30 s were also considered, but these settings were rejected due to the resulting instability of the treatment. In fact, we observed that plasma stabilization required more than 3 s, and shorter treatments were not effective or not reproducible.

2.4 Adhesive-joint fabrication and mechanical testing

CFRP-to-CFRP single-lap shear testing was performed to assess the effectiveness of plasma treatment to enhance the bond strength. To do this, the CFRP sheets were cut in accordance with the geometries established by the EN 1465 standard for the fabrication of single-overlapping joints (Fig. 2). For each set of plasma treatment conditions presented in Section 2.3, five SLJs were made and then tested ($N = 5$), and the mean value is reported in the results together with the related value of standard deviation.

DP490 adhesive was applied to the bond area of both substrates to be joined. A controlled thickness of adhesive (0.05 mm) was obtained using a sheet of non-stick paper with calibrated thickness. The substrates were placed into contact with a 12.5 mm overlap along the major axis. Any excess adhesive present at the interface was expelled by pressing the joint and then removed. Ad hoc fixing tables were used to ensure the perfect alignment of the two substrates and maintain their position throughout the week required for the complete curing of the adhesive at RT.

Table 1 Summary of the surface treatments carried out on the CFRP substrates

Surface treatment	Description	
Degreasing	Acetone wiping	
Abrasion	Acetone wiping + Scotch-Brite™ MX-SR + Acetone wiping	
Peel ply	Peel-ply removal from the top surface	
Plasma	Acetone wiping + plasma discharge with various set up parameters	
	Power (W)	50, 100, 150
	Exposure time (s)	60, 180, 300
	Gas	Air, O_2, Ar, N_2

Tensile shear strength (TSS) testing of the joints was carried out to failure at a crosshead displacement rate of 1.3 mm/min using an Instron 8802 Universal Testing machine equipped with a 50-kN load cell. The shear strength τ was calculated using the following equation:

$$\tau = \frac{F}{A_0} \quad (1)$$

where F represents the ultimate load at failure and A_0 is the initial overlap area (i.e., 25 × 12.5 mm^2).

A grip area of 25 × 25 mm^2 was ensured. Shims having the same thickness as the specimens were placed at the grip areas, in order to align the bond area along the centerline between the grip faces.

It should be noted that in the case of plasma-treated surfaces, the adhesive bonding—as well as all surface characterizations—was carried out within 15 min of treatment, in order to exclude its decay.

2.5 Roughness assessment

Morphological analysis and roughness measurements were carried out by means of a Zeta20 3D (Zeta Instruments, USA) optical profilometer. 3D images were acquired using a × 20 magnification objective, with a single field of view of 664 × 498 μm^2. The roughness parameter S_q (as well as classical S_a) has been extracted from the images, according to ISO 25178, which is suitable for characterizing anisotropic composite materials. Nine measurements have been done for each sample ($N = 9$), in order to achieve average values and related standard deviations.

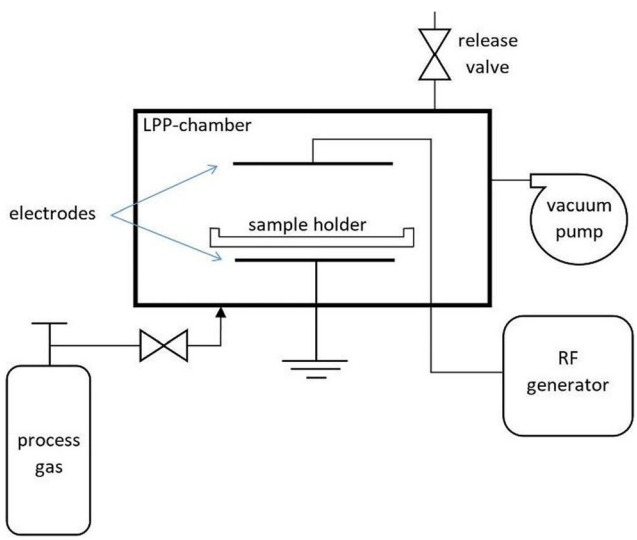

Fig. 1 Operating scheme of the LPP device employed for surface treatments

2.6 Surface chemical state

X-ray photoelectron spectroscopy (XPS) analyses were performed using a Kratos Axis Ultra^{DLD} spectrometer, equipped with a monochromatic Al Kα source (1486.6 eV) operating at 15 kV and 20 mA. All analyses were carried out on a 300 × 700 μm^2 area. Wide scans were acquired by collecting the low-resolution signals (pass energy of 160 eV and steps of 1.0 eV). High-resolution narrow scans were performed at a pass energy of 20 eV and steps of 0.1 eV. Data acquisition was carried out in UHV conditions, maintaining a base pressure below 6×10^{-9} mbar in the analysis chamber.

All spectra were charge calibrated to the main line of the C 1s spectrum (adventitious carbon), setting its binding energy value equal to 284.8 eV. Spectra were analyzed using CasaXPS software (version 2.3.18). Peak deconvolution and data fitting were carried out using Shirley-type background and Gauss-Lorentz profiles.

2.7 Surface free energy

To evaluate the surface free energy (SFE) of the substrates and appreciate its rise after vacuum plasma treatment, Wu's energy model was adopted [21, 22]. This model is successfully applicable to relatively flat surfaces and is widely used to characterize materials having low-surface energy, as with polymer or composite substrates. According to this model, by dividing the surface energy at the solid-vapor interface γ_{SV} and at the liquid-vapor interface γ_{LV} into their polar and dispersive parts (see corresponding p and d superscripts), it is possible to calculate the surface energies using a harmonic mean:

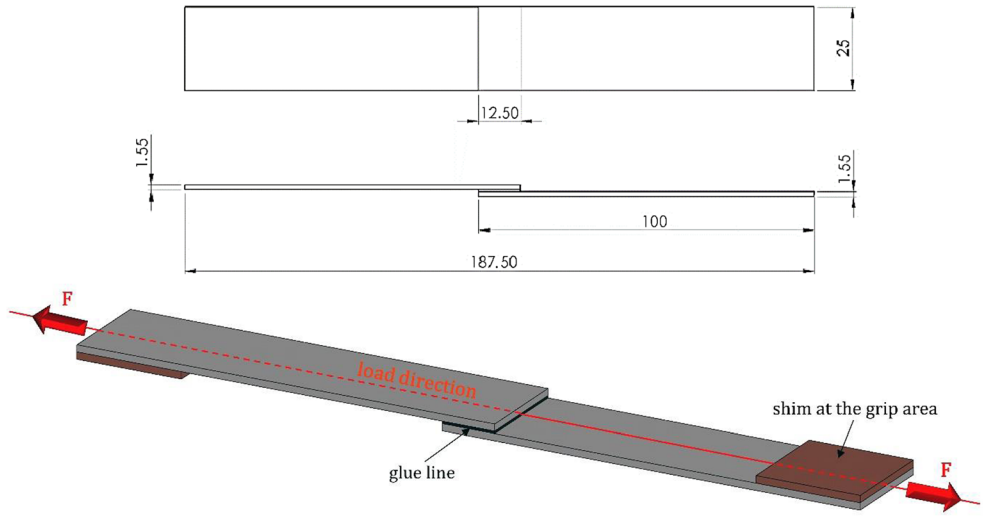

Fig. 2 SLJ geometry according to EN 1465 (values in mm) and schematic of the TSS test

$$\gamma_{SL} = \gamma_{SV} + \gamma_{LV} - 4\left(\frac{\gamma_{SV}^{d}\cdot\gamma_{LV}^{d}}{\gamma_{SV}^{d} + \gamma_{LV}^{d}} + \frac{\gamma_{SV}^{p}\cdot\gamma_{LV}^{p}}{\gamma_{SV}^{p} + \gamma_{LV}^{p}}\right) \quad (2)$$

This, combined with Young's Eq. (3),

$$\gamma_{LV}cos\theta = \gamma_{SV} - \gamma_{SL} \quad (3)$$

provides the following expression:

$$\left(\frac{\gamma_{SV}^{d}\cdot\gamma_{LV}^{d}}{\gamma_{SV}^{d} + \gamma_{LV}^{d}} + \frac{\gamma_{SV}^{p}\cdot\gamma_{LV}^{p}}{\gamma_{SV}^{p} + \gamma_{LV}^{p}}\right) = \gamma_{LV}(1 + cos\theta) \quad (4)$$

where θ is the contact angle of liquid measured at the triphasic point.

The static-θ measurements were performed with sessile drop technique, using two different test liquids: deionized water and diiodomethane (CH_2I_2). Indeed, the former has a prominent polar behavior, whereas the latter is completely non-polar. Specific CFRP laminates were dedicated to this test, each treated with a different LPP condition. The measurements were performed with an Attension Theta Lite optical tensiometer, depositing on each substrate five droplets per liquid and acquiring a total of ten values of θ (right and left). A constant droplet volume of 3 μL and 2 μL was used for H_2O and CH_2I_2 respectively, to address the different density of the two liquids and thus prevent variations of the droplet shape due to gravity [23, 24]. The captured images were then digitized using the dedicated software, One Attension. The total surface tension of the two test liquids γ_{LV} and their polar γ_{LV}^{p} and dispersive γ_{LV}^{d} components are known and are reported in Table 2. The contact angle of both liquids on the solid surface was determined and, consequently, polar γ_{SV}^{p} and dispersive γ_{SV}^{d} fractions, whose sum gives the total surface energy γ_{SV} of the solid.

3 Results and discussion

3.1 Adhesive-joint strength

As said previously, this study aims at investigating the effects of cold-plasma surface treatment on CFRP substrates by varying the most relevant parameters of the process. Mechanical tests highlighted an increase in shear strength of the adhesive bonded joints thanks to the use of plasma treatment if compared to traditional preparations, such as abrasion or peel ply. However, the improvements in performance observed with the plasma-treated joints are closely related to the power-time-gas combinations adopted during the process. Hence, the need to investigate a large number of treatment conditions by combining parameters, since—for instance—an increment of the exposure time, and perhaps even adopting a high power, does not necessarily entail the possibility of obtaining the best result.

The two traditional pre-bonding methods were firstly tested and TSS of the abraded joints stood at 18.83 ± 0.31 MPa, whereas for the peel ply, it was only 11.93 ± 0.51 MPa. Hence, in Table 3, the results of shear strength measurements for the different plasma treatment conditions are reported, with the indication of the range of maximum relative differences of the means against the abrasion and peel-ply treatments.

The errors associated with the means are the standard deviations of the measurements. The last three columns in

Table 2 Polar, dispersive, and total surface tension of the test liquids used

Liquid	γ_{LV}^{p} (mN/m)	γ_{LV}^{d} (mN/m)	γ_{LV} (mN/m)
H_2O	51	21.8	72.8
CH_2I_2	0	50.8	50.8

Table 3 Significant results of shear strength measurements for the different plasma treatment conditions. The relative differences are those of the means against the abrasion and peel-ply controls

Gas		P (W)	t (s)	Shear strength τ (MPa)	τ_{max}-τ_{min} (MPa)	Range of difference vs abrasion control (%)	Range of difference vs peel-ply control (%)
Air	τ_{max} @	150	60	27.26 ± 0.67	11.74	+ 44.7 ÷	+ 128.4 ÷
	τ_{min} @	50	180	15.52 ± 0.93		− 17.6	+ 30.1
Oxygen	τ_{max} @	150	300	26.69 ± 0.22	4.36	+ 41.7 ÷	+ 123.7 ÷
	τ_{min} @	100	300	22.33 ± 1.11		+ 18.6	+ 87.1
Argon	τ_{max} @	50	180	26.02 ± 0.51	5.74	+ 38.1 ÷	+ 118.0 ÷
	τ_{min} @	50	300	20.28 ± 1.07		+ 7.69	+ 70.0
Nitrogen	τ_{max} @	150	300	25.51 ± 0.54	5.74	+ 35.5 ÷	+ 113.8 ÷
	τ_{min} @	50	60	19.77 ± 1.58		+ 5.0	+ 65.7

Table 3 highlight the spread of values in the obtained measurements. In particular, the two rightmost columns allow one to compare this spread with the abrasion and peel-ply controls, respectively, against which improvements are represented by "+" signs, while a "−" sign represents a decrease in performance. However, owing to low efficiency of the peel-ply preparation, from then on, it was decided to compare all the results obtained with LPP treatments to the case of abrasion only. The improvement in joint performance is more evident in those cases where Air and O_2 (+ 44.7% and + 41.7% respectively) are used as process gases, followed by Ar (+ 38.1%) and N_2 (+ 35.5%). This increase is referred to the most successful power-time combination found for each gas. In fact, thanks to an overview of all the treatment combinations performed, it is clear that the mechanical behavior of the adhesively bonded joints is mostly influenced by the process gas used, which is the information stressed in Fig. 3.

The histograms presented in Fig. 3 show the same mean and error data as in Table 3, grouped in such a way as to stress the trends emerging for the different gases used. Generally speaking, it appears that at low power (50 W), oxygen scores are always best or second best, while the second best fluctuates between argon and nitrogen among the different combinations of power and time, with air always scoring the worst. Conversely, at intermediate (100 W) and high power (150 W), air seems to be the most effective gas at all times, with oxygen usually scoring second. In particular, at the highest power (150 W), nitrogen performs better than argon, different from the intermediate power case (100 W).

Statistical analysis by Pearson's correlation factors (f_P) was then carried out, in order to evaluate, for each gas, whether and how much the variations of power input and process duration affect shear strength. The results obtained are reported in Table 4: the relationship is to be intended as "weak" for $f_P < 0.3$, "moderate" if between 0.3 and 0.7, and "strong" for f_P ranging from 0.7 to 1.

Hence, with an air-plasma treatment (Fig. 3a), CFRP joints present a high strength when the process involves a high power (≥ 100 W), even if the exposure time is limited (60 s). By contrast, the use of a lower powered air-plasma is not sufficient to determine an increase in mechanical performance: almost no relevant variations in the joint strength were obtained at all compared to the reference (abraded), even when prolonged treatment times are used. Thus, it follows that, for an air-plasma treatment, the power value chosen for the process seems to play a more meaningful role (power input and strength statistically resulted in a strong direct relationship, with a $f_P = 0.88$), while the duration of exposure, however, can be limited to obtain excellent results.

When argon was used as process gas (Fig. 3c), the best mechanical response was obtained from joints treated using a combination of low power (50 W) and mid-high time (180 s). However, it was sufficient simply to increase treatment time to 300 s to determine a considerable loss of mechanical resistance. Despite this, adopting a power input of 100 W, the shear strength of the joints presented a trend that was almost constant through time, with low values of standard deviation especially when time did not exceed 180 s. However, even adopting Pearson's statistical analysis, to identify uniquely an overall trend of the mechanical response with process parameter is not easy, since the correlation between shear strength and the two process parameters investigated resulted very weak in both cases.

Then, with a nitrogen-plasma treatment, mechanical strength increased with the rise of both power and exposure-time values (Fig. 3d). In particular, a minimum shear strength corresponded to the softer treatment condition (at 50 W for 60 s), while the maximum was obtained with the most invasive combination (150 W, 300 s). Both power and time parameters statistically result in a direct relationship with shear strength, although time input seems to have stronger influence on performance variations. It should also be noted that an increase of the treatment duration generally entailed a relevant reduction in result dispersion, which became small in all the cases in which an exposure of 300 s was set.

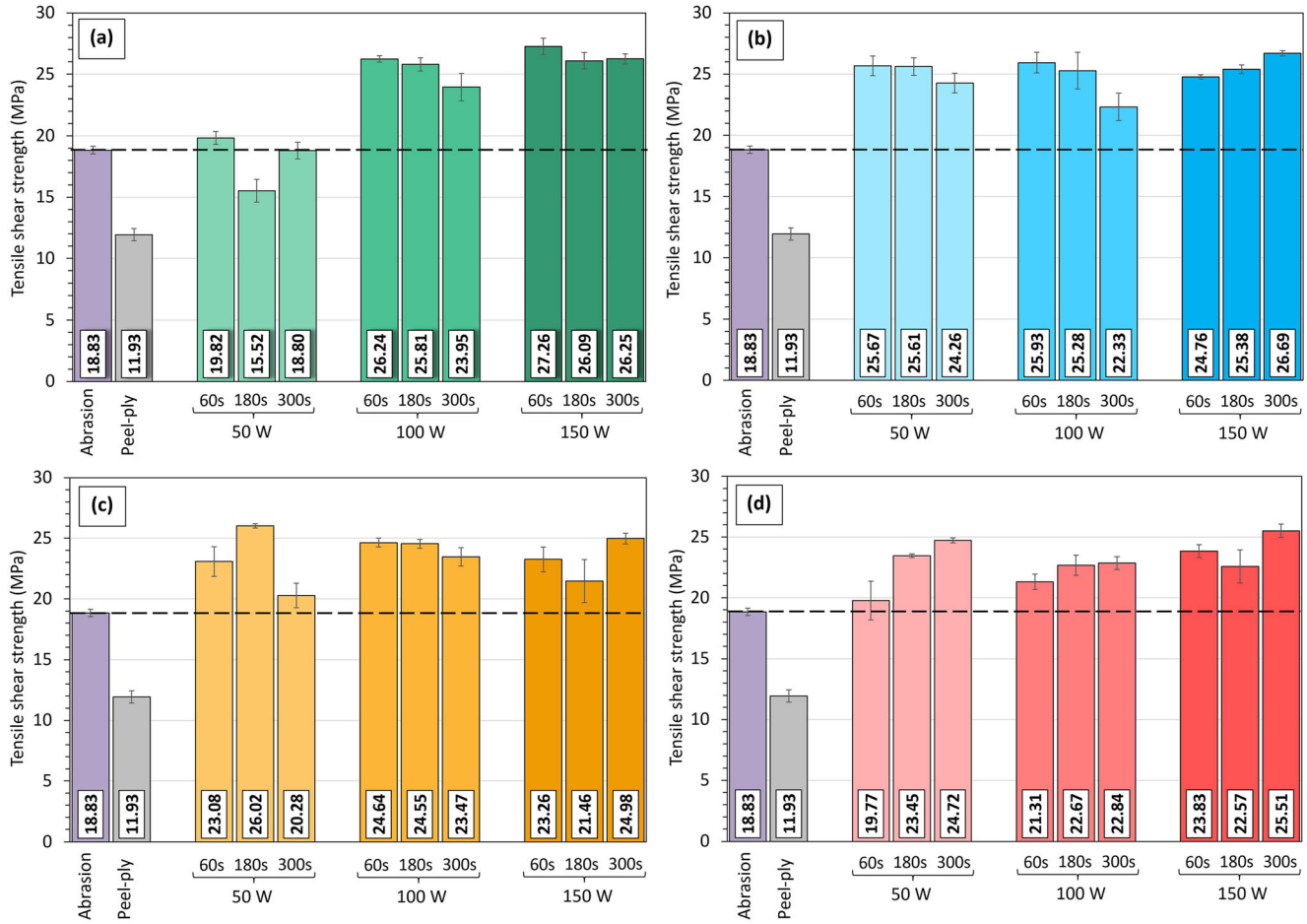

Fig. 3 Histogram plots of the TSS test results obtained with different plasma treatment conditions of power and exposure time, grouped according to the plasma process gas: **a** air, **b** oxygen, **c** argon, and **d** nitrogen. Black dotted line represents the reference mean value of shear strength presented by the abraded control joints

Finally, TSS tests of oxygen-plasma-treated samples witnessed a minor variation of mechanical performance when varying both power and time inputs (Fig. 3b). In particular, these results highlighted a limited difference between the best and the worst value of shear strength (only 4.4 MPa ca.) obtained with this gas. This reflects the fact that, in general, use of oxygen may entail a more manageable and less fallacious process, since effectiveness of the treatment might not be affected by any setting error of the operator. However, always referring to Fig. 3, it is evident that—even if the most effective treatment corresponded to the highest values of both parameters—excellent results can also be reached adopting a brief low-powered process. And this is especially advantageous when high productivity is required.

In view of the above results, it can be concluded that the shear strength of the joints confirms the importance of the vacuum plasma as a pre-bonding treatment for CFRP substrates. The effectiveness of plasma treatment is highlighted also observing the overlap fracture surfaces of the joints, as shown in Fig. 4, which is illustrative of the failure mode obtained after the two aforesaid traditional treatments and the best plasma ones. In Fig. 4, one can see a clear evolution from states of complete de-adhesion for the surfaces where the peel ply has been removed to an almost completely de-cohesive mode for plasma-treated substrates. In this regard, as discussed in the following sections, the reason for this behavior is to be sought both in a morphological modification and in the surface activation state brought about by plasma. This activation involves both an increase of the wettability properties of substrate and a change of the surface chemical state with generation of polar groups at interphase that let adherend create stable bonds with the adhesive. Thus, because from mechanical data, it was not possible to draw a clear conclusion, more experiments were carried out, which are described and discussed in the following.

3.2 Morphological effect of plasma on CFRP substrates

Starting from the experimental findings of the mechanical characterization, surface morphological analyses were performed on the degreased-only (representing the as-received

Table 4 Influence of the process parameters on the tensile shear strength, statistically evaluated by Pearson's correlation factor analysis

Gas	Plasma-parameter influence on TSS (Pearson's correlation factor, f_P)	
	Power	Time
Air	Strong (0.88)	Weak (− 0.15)
Oxygen	Weak (0.15)	Moderate (− 0.36)
Argon	Weak (0.03)	Weak (− 0.18)
Nitrogen	Moderate (0.33)	Moderate (0.68)

surface, only wiped with acetone and not further treated), abraded, and peel-ply substrates as well as on those plasma-treated samples among those reported in Table 3 for which only the best and worst plasma conditions have been selected. In this way, it was also possible to correlate the choice of plasma power and time to creation of different topological structures on the CFRP surfaces differently treated. In this regard, Fig. 5 reports 2D top-view optical images acquired simultaneously, for a given gas, on the CFRP surfaces plasma-treated according to the worst (left) and the best (right) power-time settings; below each image, the corresponding treatment conditions and the related S_q-values measured are reported. It is clear that the extent of surface modification is strictly related to the power-time combination used, and this behavior confirms the previous considerations about the different significance of power and time combinations on the different processing gas.

In general, regardless of the gas used, the best plasma-treated CFRP presented a surface conformation which was rich in crater-shaped valleys. To understand this type of surface modification, it should be considered that the plasma consists of electrons, ions, photons, and molecules having high kinetic energy, which is furtherly enhanced in the vacuum ambient of the processing chamber [25]. These high-energy particles actually bombard the surface of the substrate, thus leaving the sign of their impact on it, which is the base of plasma-etching phenomenon observed by Tang et al. also on activated carbon fibers [13]. It should be noted that the highest power (150 W) works best at increasing the S_q roughness of the substrate when air, oxygen, and nitrogen are used to generate the plasma atmosphere. In particular, an exposure of only 60 s to a 150-W air-plasma was enough to reach an average S_q of 0.90 μm, which is close to that found on the abraded surface (0.92 ± 0.10 μm). Instead, although using air for a longer time, low plasma power did not allow us to obtain a significant modification of the surface: for the treatment with air at 50 W–180 s combination, S_q was only 0.52 μm—i.e., less than that measured on the sample before treatment (0.76 μm). However, also in this case, tiny craters were created due to the etching effect, as visible in the inset to Fig. 5a on the left (a1) surface, acquired with a × 10 magnification. A similar behavior was also observed on nitrogen-plasma-treated surfaces (see inset to Fig. 5d, left half, i.e., d1), where both the most powerful treatment and the least invasive one originated surfaces having roughness values which were smaller (0.65 and 0.44 μm respectively) than that obtained on the only-degreased surface.

As regards, the results obtained using the other process gases, oxygen-plasma, and argon-plasma generated morphologically similar surfaces both on the most and least-performing substrates. In particular, surfaces treated with O_2-plasma presented an average S_q-value of 0.87 μm at maximum power and time, and 0.75 μm reducing power to 100 W. In contrast, morphological modification of Ar-plasma-treated substrates is observable only adopting a low-powered plasma (50 W); it was also interesting to note that maximum roughness (0.77 μm) is not much higher than that before treatment and—as well as mechanical strength—it was obtained with an

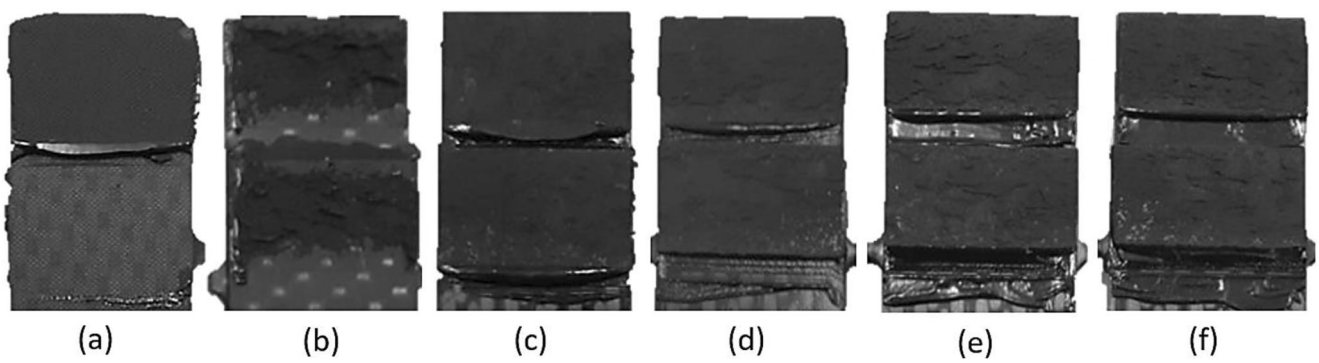

Fig. 4 Fracture areas of joints adhesively bonded after the following treatments: **a** peel-ply removal, **b** abrasion, **c** air-plasma, **d** oxygen-plasma, **e** argon-plasma, **f** nitrogen-plasma. The cases of plasma treatments shown are for the most performing power-time settings

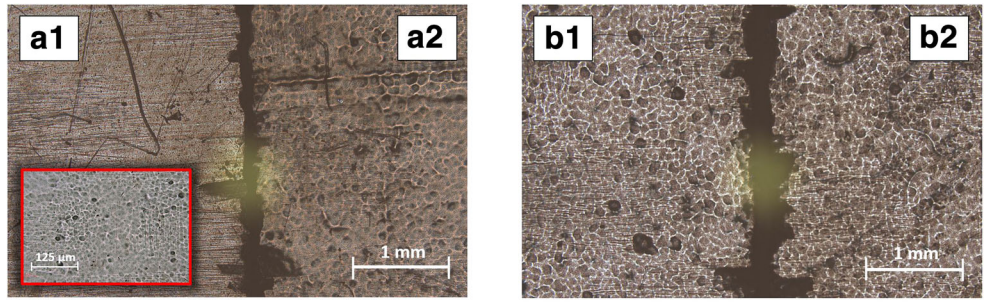

	P (W)	t (s)	S_q (µm)
(a1)	50	180	0.52 ± 0.48
(a2)	150	60	0.90 ± 0.06

	P (W)	t (s)	S_q (µm)
(b1)	100	300	0.75 ± 0.05
(b2)	150	300	0.87 ± 0.14

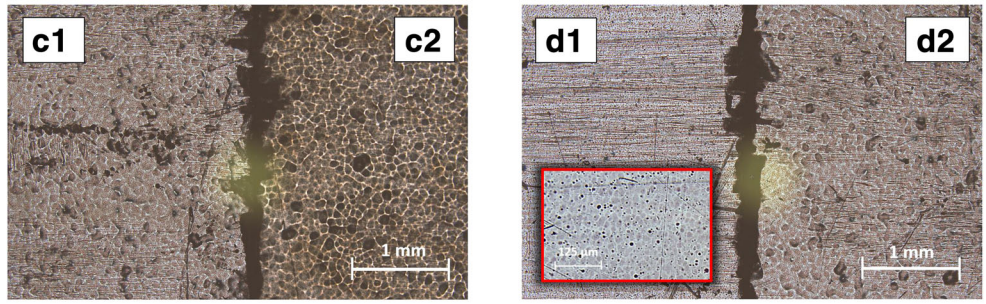

	P (W)	t (s)	S_q (µm)
(c1)	50	300	0.66 ± 0.06
(c2)	50	180	0.77 ± 0.04

	P (W)	t (s)	S_q (µm)
(d1)	50	60	0.44 ± 0.04
(d2)	150	300	0.65 ± 0.35

Fig. 5 Top-view 2D optical images of the CFRP substrates acquired with × 2.5 magnification objective. The substrates were treated with: (a1, a2) air-plasma, (b1, b2) oxygen-plasma, (c1, c2) argon-plasma, (d1, d2) nitrogen-plasma. The half images on the left and on the right show the surface of the worst (e.g., a1) and the best (e.g., a2) plasma treatment conditions, respectively. In the tables on the bottom of the images, the respective S_q roughness parameter values are also reported

intermediate treatment duration of 180 s, whereas the minimum one (0.65 µm) increasing the exposure time to 300 s.

In view of these results, one can conclude that surface modification due to plasma plays a prominent role in the mechanical interlocking between adhesive and CFRP substrate, thanks to both an increase—in many cases—of the surface roughness and above all to a modification of the texture of the surface. This is clear when comparing the degreased-only control surface (Fig. 6a) to the plasma-treated surfaces: even when the term of comparison is the worst plasma-treated surface—such as in cases a1 or d1—where on the larger scale (× 2.5 magnification), the same horizontal lines due to the original fabrication process of the piece appear, still on the microscale (× 10 magnification), the plasma-treated surface shows tiny craters, whereas the control only keeps showing the same horizontal lines. These horizontal lines are related to the impression of vacuum bag during the CFRP manufacturing.

Roughness results are in accordance with trend of the shear strength. However, this analysis also proved that improvement in mechanical performance of the joints is a consequence of concurrent causes and effects, such as surface activation and thus chemical interaction between adhesive and substrate, and absence of contamination on the surface to be adhesively bonded; indeed, such consideration, together with the morphological assessments carried out, allowed us to find a possible explanation of the mechanical behavior presented by the joints bonded after peel-ply removal. In this regard, Fig. 6b

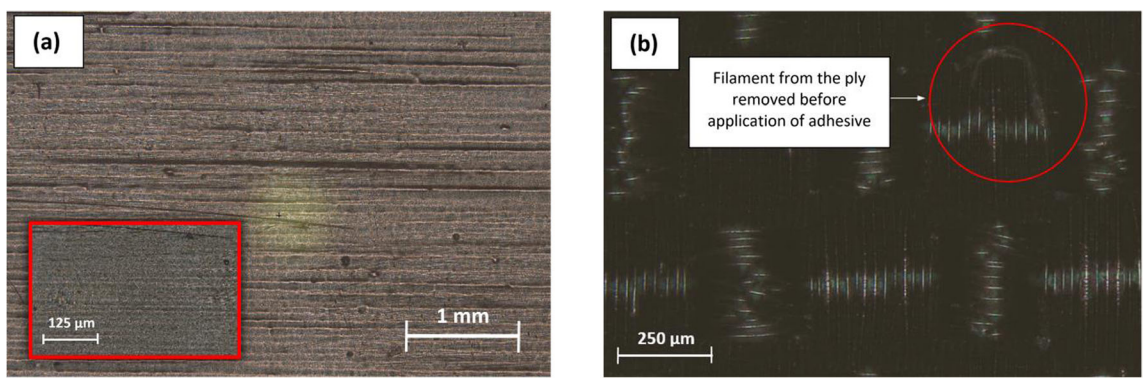

Fig. 6 **a** Degreased-only control surface and **b** detail of the surface effect of the peel-ply removal from the CFRP substrate: topography is repetitive and shows a strong increase in roughness, but traces of contaminant are easily detectable and lead to a reduction of the adhesive capability of the substrate

shows an image of such surface immediately after having removed the fabric ply, i.e., in that condition before the adhesive is applied. Traces of polyester filaments are clearly visible since they presumably remained trapped in epoxy matrix during consolidation of the composite; obviously, these filaments of releasing material are detrimental to adhesion and may undermine the effect of mechanical interlocking (in this case, S_q value was 11.05 ± 1.91 μm), as indeed highlighted during mechanical tests.

3.3 Evaluation of surface chemistry through XPS

XPS analyses of CFRP were carried out before and after plasma treatment in order to investigate what chemical modifications occur on surface and how these contribute to the observed wettability properties. Wide scan acquisitions allowed to identify the chemical composition of the investigated CFRP substrates, within a 10-nm depth, comparing the degreased-only control surface and the plasma-treated samples whose surfaces were modified using the best parameter-settings found, for each gas, during the mechanical characterization.

As shown in Table 5, independently on the used process gas, plasma treatment determines an increase in oxygen content together with a decrease of the C 1s peak, i.e., an oxidative effect that is reflected in an increase of the oxygen/carbon ratio (with a + 242.9% using oxygen, + 207.1% with air, and + 178.8% and + 100% with nitrogen and argon respectively), with respect to the untreated CFRP surface. Thus, starting from this low-resolution analysis, two specific energy regions were selected, providing a targeted survey aimed at photographing the specific effect of treatment in terms of oxidation and activation of the CFRP substrates. These regions are located around C 1s (280 ÷ 294 eV) and O 1s (528 ÷ 540 eV) peaks. The shape of both the carbon and the oxygen peaks varied appreciably from one substrate to another, depending, for each gas, on the surface modification involved by using the specific optimized set of parameters.

Deconvolution of C 1s peak made it possible to identify a number of carbon components (Fig. 7a) related to the following: single bond between carbon and carbon or carbon and hydrogen (C–C, C–H) positioned at 284.8 eV, carbon singly bound to nitrogen (C–N) at 285.9 eV and with oxygen (C–O) at 286.6 eV. Furthermore, a peak corresponding to carbon forming two single bonds or one double bond with oxygen (O–C–O, C=O) was recognized at 287.8 eV, while carboxyl group (O–C=O) was found at 289.5 eV [26, 27]. Thus, as shown by deconvolving C 1s, before vacuum plasma treatment C–C/C–H bonds are predominant, whereas treated substrates present a simultaneous decrease of concentration of these species and rise of peaks corresponding to bonds between carbon and oxygen. This suggests that—regardless of the type of process gas used—plasma treatment changes the surface chemical state of the CFRP substrates, forming new functional groups as a result of the break of the original single bonds C–C or C–H; indeed, comparing pre- and post-treatment conditions, the decreasing trend of these bonds is believed to be the direct effect of increasing of various oxidative reactions that occurred during plasma treatment, which involve generation of single or double bonds between oxygen and carbon atoms. Obviously, this behavior is emphasized when optimized O_2-plasma treatment was performed, which represents the clearest case in which a substantial reduction of C–C/C–H bonds (− 43.4% compared to the reference) is followed by an equally clear increment of oxidized species. Indeed, free radicals can be created on the treated surfaces, which can then couple with active species from the plasma environment; these reactions are believed to be essential for the changes in the surface functionalities [13, 28].

High-resolution survey on O 1s spectrum and subsequent deconvolution of this peak also highlighted the presence of two different chemical species (Fig. 7b), which can be considered as a confirmation of the high activation and oxidation of the CFRP plasma-treated substrate: a first one, at about 531.8 eV, interpreted as oxygen making two single bonds with carbon (C–O–C) or carbon forming one single bond with a hydroxyl (–OH); and a second one (at 532.8 eV) corresponding to an O–C=O group. Always referring to Table 5, it should be noted that the latter seems to decrease after all plasma treatment, whereas percentage of the former increases; however, the reason for this behavior is believed to be related to the fact that the number of C–OH bonds rises more steeply

Table 5 Atomic percentages of oxygen and carbon, and related O/C ratio, obtained through XPS analysis in **a** survey mode and area percentage of each chemical species quantified from deconvolution of **b** C 1s and **c** O 1s peaks

Surface treatment	Atomic percentage (%)			Area percentage (%)						
	O 1s [(a)]	C 1s [(a)]	O/C ratio	C–C C–H[(b)]	C–N[(b)]	C–O[(b)]	O–C–O C=O[(b)]	O–C=O[(b)]	C–OH C–O–C[(c)]	O–C=O[(c)]
Degreasing	12.07	87.93	14	70.61	14.52	9.88	2.58	2.41	52.26	47.74
Air-plasma	30.13	69.87	43	50.26	16.86	21.27	6.12	5.03	70.35	29.65
Oxygen-plasma	32.35	67.65	48	43.37	19.37	24.48	8.44	4.35	67.27	32.73
Argon-plasma	21.59	78.41	28	57.55	14.14	16.05	5.77	6.48	61.10	38.90
Nitrogen-plasma	28.00	72.00	39	47.75	19.16	21.06	6.98	5.06	69.59	30.41

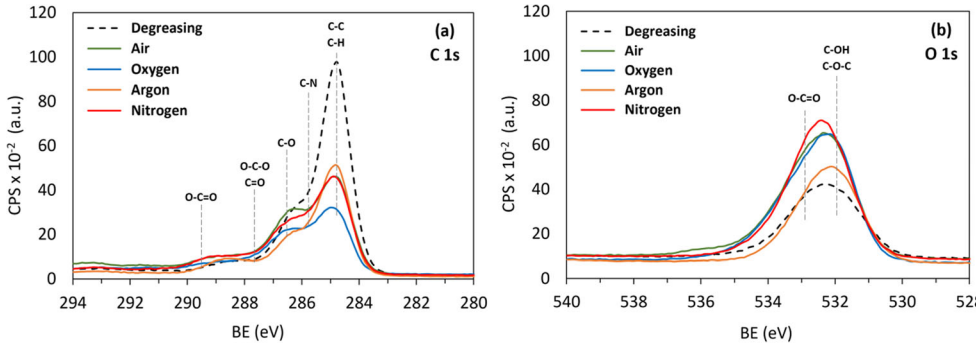

Fig. 7 Comparison of the XPS spectra acquired before and after vacuum plasma treatment of the CFRP substrates: **a** C 1s and **b** O 1s peaks, shown as superposition of the pre- and post-treatment curves. Each plasma-treated CFRP spectrum is referred to the power-exposure time combination which gave, with the specific process gas, the best mechanical result (see Table 3)

than the O–C=O ones, rather than to an effective decrease of this second species. Thus, similar to that found analyzing C 1s, such newly formed functional groups as well as the introduction of additional groups ensure an enhancement of the surface polarity and, consequently, could develop its hydrophilic behavior, as discussed in the following section. These increased polar groups supplied more reactive sites for interfacial bonding between the epoxy matrix of CFRP laminate and epoxy adhesive and thus could lead to an improvement of performance of the adhesively bonded joint so-treated.

3.4 Wettability and surface energy measurements

The results of measurements of CA with the two different selected probe liquids, H_2O and CH_2I_2, are presented in Table 6, where the average value of θ and related standard deviation are reported.

Based on the previous characterization, the number of plasma environments to be tested was reduced, selecting only those power conditions which allowed the adhesively bonded joints to reach the highest mechanical strength. Thus, wetting analyses were performed only on substrates treated at plasma powers of 50 W and 150 W, neglecting the case at intermediate power of 100 W. Exposure-time parameter was maintained variable between 60, 180, and 300 s. Indeed, experimental results indicated that increasing plasma treatment time is not always helpful in enhancing the wetting properties of epoxy-based composite. As comparators, abrasion and peel-ply techniques were adopted to define a reference value for both CAs and surface energy; moreover, measurements were also performed on degreased-only substrates, representing the zero-condition common to all the plasma-treated surfaces.

As shown in Table 6, all plasma treatments generally involved a reduction of CAs compared to the three references, already after the first minute of treatment, independently on both process gas and power; this reduction was more evident with deionized water droplets rather than to CH_2I_2 ones. This behavior could be related to oxidizing effect of plasma itself, which introduces or stimulates—as previously shown—the increase of polar species on the CFRP surface, developing its hydrophilicity. Indeed, as known, plasma treatment leads to an increase in surface energy of the solid invested. In this regard, the histogram of Fig. 8 reports surface energy results obtained by implementing the measured CAs to Wu's energy model, defining for each set the related polar and dispersive fractions of this quantity. Considering the case where air was used as process gas, contact angle trend followed exactly the aforesaid considerations, progressively declining with the rise of both time spent by the substrate under plasma-exposition and power set for treatment. However, it was interesting to note that maximum mechanical strength did not correspond to maximum wettability of substrate. The experimental tests highlighted this aspect also when oxygen or argon was used; in the former case, θ values of both liquids decreased with time adopting a 50-W power, but tended to progressively rise again at 150 W. It should be remembered that the highest value of mechanical shear strength was obtained with the parameter-setting 150 W-300 s, which corresponded even to the highest water-θ value reached with O_2-plasma treatment. Similarly, in the latter case (argon), maximum mechanical performance was obtained for the lower θ values at 50 W, which were not however the absolute smallest ones. Thus, by observing the experimental findings, a strict correspondence between shear strength and minimum-θ/maximum-γ_S was highlighted only on nitrogen-plasma-treated samples. Such a behavior is however not unexpected and it is to be intended as confirmation of the idea that surface wettability is a necessary, but not sufficient condition for bonding, to which it is thus not possible to uniquely relate the success of an adhesively bonded joint [29, 30].

To make comparisons among the obtained results, of course, is not easy; indeed, the study is focused on both a same type of treatment (plasma) with several experimental parameters and different treatments with different kinds of surface modifications: chemical and morphological for plasma, but mostly morphological using peel ply and abrasion. To understand and control adhesive phenomena, however, a holistic

Table 6 Results of the contact angle analysis performed on CFRP using deionized water and diiodomethane. Values related to the best plasma settings are marked in italic

Surface treatment				θ_{H_2O} (deg)	$\theta_{CH_2I_2}$ (deg)
Degreasing				82.5 ± 0.6	46.1 ± 0.4
Abrasion				79.2 ± 0.9	26.7 ± 1.5
Peel ply				50.1 ± 0.8	25.1 ± 0.6
Plasma	Gas	P (W)	t (s)		
	Air	50	60	39.0 ± 3.4	45.0 ± 1.4
			180	32.5 ± 0.5	41.7 ± 0.3
			300	29.1 ± 0.6	29.9 ± 0.8
		150	60	29.1 ± 0.1	30.0 ± 0.2
			180	28.6 ± 1.0	30.7 ± 1.2
			300	25.6 ± 0.3	31.3 ± 0.6
	Oxygen	50	60	33.9 ± 0.7	43.0 ± 0.7
			180	29.9 ± 0.5	42.0 ± 0.8
			300	27.2 ± 0.5	29.4 ± 0.6
		150	60	29.1 ± 0.1	28.3 ± 0.5
			180	32.2 ± 0.1	27.9 ± 0.1
			300	34.8 ± 0.1	29.7 ± 2.1
	Argon	50	60	51.0 ± 3.6	38.3 ± 0.5
			180	28.8 ± 1.4	37.7 ± 0.3
			300	31.7 ± 0.4	33.9 ± 0.1
		150	60	28.4 ± 0.3	38.0 ± 1.3
			180	22.4 ± 0.5	33.7 ± 3.2
			300	22.4 ± 0.8	26.2 ± 1.3
	Nitrogen	50	60	39.6 ± 1.2	45.3 ± 0.3
			180	36.8 ± 0.4	50.8 ± 1.4
			300	29.8 ± 0.1	33.8 ± 0.2
		150	60	29.2 ± 0.6	40.8 ± 1.0
			180	27.4 ± 0.2	32.6 ± 0.4
			300	25.7 ± 1.1	21.7 ± 1.2

approach is needed. As shown in Section 3.2, progressive enhancement of surface roughness and creation of a proper morphology lead to an improvement in mechanical performance of the adhesive joints, since an increase of the roughness ratio generally means enlargement of the actual contact area and, thus, of the effective interface between adhesive and substrate. But, as experimentally observed in this work and also pointed out by many authors [31, 32], to have strong adhesion, the adhesive must wet the surface and have rheological properties sufficient to penetrate within the surface irregularities. Consequently, topological evaluation cannot ignore considerations about wettability of the surface, since the non-wetting may avoid adhesive bonds from forming at all. In this regard, wetting analysis results highlighted some main characteristics of the CFRP substrates according to the specific treatment performed. Abrasion and peel ply have similar dispersive SFE components (45.7 mJ/m^2 and 46.2 mJ/m^2 respectively) but peel-ply polar contribution is almost triple (21.4 mJ/m^2) than that obtained with abrasion (7.9 mJ/m^2). Indeed, abrasion with Scotch-Brite™ MX–SR results in a surface with a non-well-balanced ratio between polar and dispersive SFE fractions, which clearly leans toward the latter, whereas polar component is low and almost the same of the only-degreased surface. On the contrary, vacuum plasma treatment creates polar groups on the surface, leading to a higher polar SFE fraction. Thus, considering that also surface topography is particularly affected by this treatment (although in a lesser extent if compared to abrasion and, even more so, peel ply), it could be concluded that the increase in TSS performance after plasma treatment is due to concomitant effects of mechanical interlocking and chemical modification of the CFRP epoxy-matrix; in other words, as statistical analysis also revealed, shear strength obtained on plasma-treated SLJs is strictly influenced by both surface roughness (the related Pearson's coefficient is almost one) and increase of the O/C ratio (f_P= 0.53). Hence, the experimental findings suggested that predominating adhesion mechanisms in the shear strength of epoxy-bonded CFRP substrates are those which represent a premise for steady chemical interactions between surface and adhesive, i.e., chemical bonding.

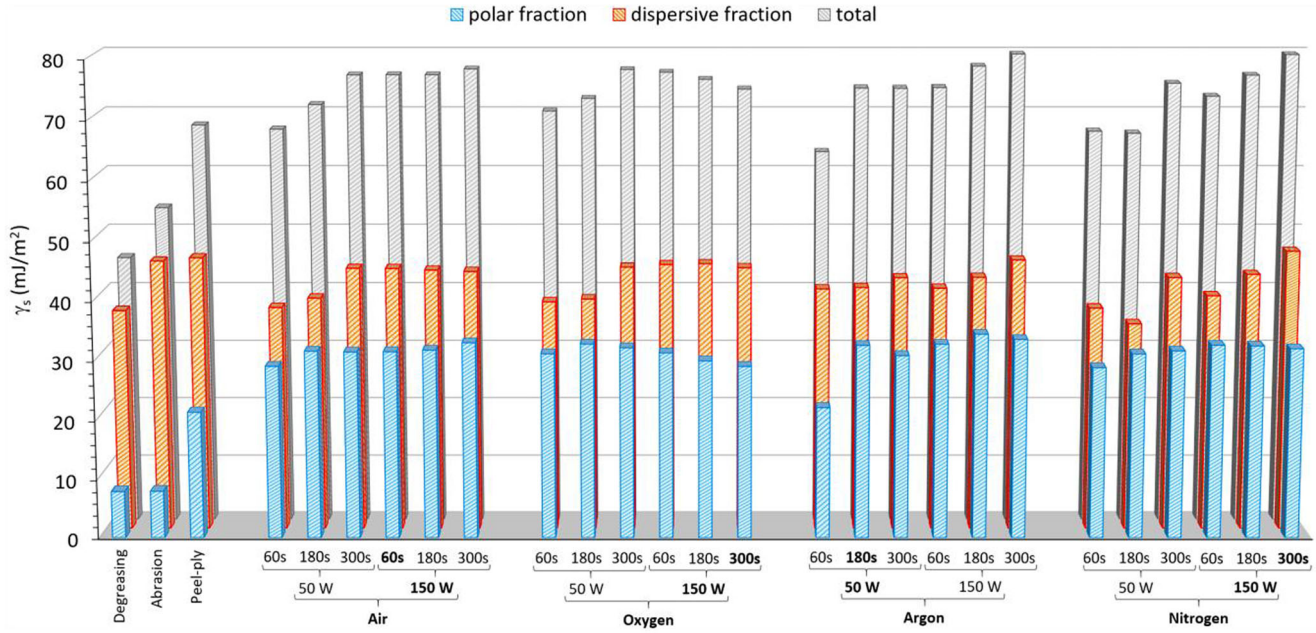

Fig. 8 Representation of the polar, dispersive, and total fractions of the SFE calculated with Wu's energy model implemented with the CAs acquired on the degreased-only, abraded, peel-ply, and plasma-treated CFRP surfaces. Values related to the best plasma settings are marked in bold

4 Conclusions

In this research, a comprehensive experimental campaign was carried out in order to point out and discuss the effects of various pre-bonding techniques such as abrasion, peel-ply, and vacuum cold-plasma treatments, especially focusing on the engineering of the latter considering four different process gases (air, oxygen, argon, and nitrogen), at different powers and exposure times. At first, mechanical tests were performed on joints manufactured by overlapping of two CFRP substrates, whose surfaces were treated using the aforementioned techniques. From the mechanical characterization—which involved 36 different plasma-treatment conditions—it was possible to identify, for each gas, both the optimal plasma combination of power and exposure time, which ensured reaching the highest shear strength of the joints; and how and how much these two inputs affect the process. Considering also all further analyses of contact angle, morphology and chemical state of the surfaces for a subset of the most significant combinations of plasma treatment, performed on the CFRP substrates to be adhesively joined, all the following conclusions can be drawn:

- When using the abraded surface as the reference, using plasma with air, oxygen, argon, or nitrogen, it was possible to enhance shear strength up to 44.7%, 41.7%, 38.1%, and 35.5% respectively; every joint so-treated presented almost-complete cohesive failure, which confirmed the success of the surface preparation;
- Use of air as process gas to obtain an increase of mechanical performance required adoption of mid-high powers ($\geq$ 100 W) even for short exposure times;
- Oxygen-plasma resulted into a more robust process, since effectiveness of the treatment seemed not to be exceedingly affected by power-time settings: actually, although highest shear strength corresponded to the highest values of both power and time, effective results were also obtained with short time and low power processes.
- Using argon to generate plasma, adoption of an intermediate power of 100 W allowed us to obtain mechanical results that were more stable versus the exposure time; however, the best performance seems to appear at 180 s and 50 W treatment;
- In general, the mechanical strength of joints treated with a nitrogen-plasma increased with the parallel rise of power and time. Indeed, the minimum strength appears with a combination of 50 W–60 s and the maximum strength appears at 150 W–300 s;
- Morphological assessment showed an effective modification of the surface, with creation of crater-shaped valleys which increment the action of mechanical interlocking between adhesive and adherend; also roughness (i.e., the parameter S_q) increases, following a trend which seems to be in accordance with shear strength, even if its value never exceeded that presented on the abraded sample and actually in some cases was below that obtained before plasma treatment. Considering that such behavior was observed especially with air and mostly nitrogen after a not so prolonged

stay (180 and 60 s respectively) at low power (50 W), one can speculate that plasma initially made the surface smoother than the original substrate.

– Wetting analysis allowed us to determine that plasma treatments also result in a remarkable increase of the polar component of the SFE and, thus, in an enhancement of the capability of the substrate to be wet by the adhesive; in other terms, vacuum plasma makes the resin penetrate into surface irregularities, generating stable chemical bonds with the adherend. As resulted from the XPS analyses of the CFRP substrates treated at the best conditions, activation and rise in hydrophilicity of the surface could be related to the oxidizer effect of plasma itself, which appears with a strong increase of the oxygen/carbon ratio and a deep stimulation of polar species produced from the bond between oxygen and carbon (e.g., C–O, C=O, O–C–O, O–C=O). Obviously, this behavior was emphasized when O_2 was used as processing gas.

Thus, having found the optimal cold-plasma treatment conditions, this work represents the preliminary basis for a subsequent investigation, focused on the behavior of so-treated joints when they are subjected to aging.

References

1. Friedrich K, Almajid AA (2013) Manufacturing aspects of advanced polymer composites for automotive applications. Appl Compos Mater 20:107–128. https://doi.org/10.1007/s10443-012-9258-7
2. AL-Zubaidy H, Zhao XL, Al-Mihaidi R (2011) Mechanical behaviour of normal modulus carbon fibre reinforced polymer (CFRP) and epoxy under impact tensile loads. Procedia Eng 10:2453–2458. https://doi.org/10.1016/j.proeng.2011.04.404
3. Morioka K, Tomita Y, Takigawa K (2001) High-temperature fracture properties of CFRP composite for aerospace applications. Mater Sci Eng A 319–321:675–678. https://doi.org/10.1016/S0921-5093(01)01000-0
4. Kumar SB, Sridhar I, Sivashanker S, Osiyemi SO, Bag A (2006) Tensile failure of adhesively bonded CFRP composite scarf joints. Mater Sci Eng B 132:113–120. https://doi.org/10.1016/j.mseb.2006.02.046
5. Kanerva M, Saarela O (2013) The peel ply surface treatment for adhesive bonding of composites: a review. Int J Adhes Adhes 43. https://doi.org/10.1016/j.ijadhadh.2013.01.014
6. Holtmannspötter J, Czarnecki JV, Wetzel M, Dolderer D, Eisenschink C (2013) The use of peel ply as a method to create reproduceable but contaminated surfaces for structural adhesive bonding of carbon Fiber reinforced plastics. J Adhes 89:96–110. https://doi.org/10.1080/00218464.2012.731828
7. Schweizer M, Meinhard D, Ruck S, Riegel H, Knoblauch V (2017) Adhesive bonding of CFRP: a comparison of different surface pretreatment strategies and their effect on the bonding shear strength. J Adhes Sci Technol 31:2581–2591. https://doi.org/10.1080/01694243.2017.1310695
8. Davis M, Bond D (1999) Principles and practices of adhesive bonded structural joints and repairs. Int J Adhes Adhes 19:91–105. https://doi.org/10.1016/S0143-7496(98)00026-8
9. Wegman RF, Van Twisk J (2013) Surface preparation techniques for adhesive bonding, 2nd edn. Elsevier, New York
10. Ebnesajjad S, Landrock AH (2014) Material surface preparation techniques. Adhes Technol Handb, pp 37–46. https://doi.org/10.1016/B978-0-8155-1533-3.50006-2
11. Tang L, Kardos JL (1997) A review of methods for improving the interfacial adhesion between carbon fiber and polymer matrix. Polym Compos 18:100–113. https://doi.org/10.1002/pc.10265
12. Montes-Morán MA, Martínez-Alonso A, Tascón JMD, Young RJ (2001) Effects of plasma oxidation on the surface and interfacial properties of ultra-high modulus carbon fibres. Compos A Appl Sci Manuf 32:361–371. https://doi.org/10.1016/S1359-835X(00)00109-3
13. Tang S, Lu N, Wang JK, Ryu S-K, Choi H-S (2007) Novel effects of surface modification on activated carbon fibers using a low pressure plasma treatment. J Phys Chem C 111:1820–1829. https://doi.org/10.1021/jp065907j
14. Shanahan MER, Bourges-Monnier C (1996) Effects of plasma treatment on the adhesion of an epoxy composite. Int J Adhes Adhes 16:129–135. https://doi.org/10.1016/0143-7496(95)00028-3
15. Li R, Ye L, Mai Y (1997) Application of plasma technologies in fibre-reinforced polymer composites: a review of recent developments. Compos A Appl Sci Manuf 28:73–86. https://doi.org/10.1016/S1359-835X(96)00097-8
16. Tendero C, Tixier C, Tristant P, Desmaison J, Leprince P (2006) Atmospheric pressure plasmas: a review. Spectrochim Acta B At Spectrosc 61:2–30. https://doi.org/10.1016/j.sab.2005.10.003
17. D'Agostino R, Favia P, Oehr C, Wertheimer MR (2005) Low-temperature plasma processing of materials: past, present, and future. Plasma Process Polym 2:7–15. https://doi.org/10.1002/ppap.200400074
18. Molitor P, Barron V, Young T (2001) Surface treatment of titanium for adhesive bonding to polymer composites: a review. Int J Adhes Adhes 21:129–136. https://doi.org/10.1016/S0143-7496(00)00044-0
19. He P, Chen K, Yu B, Yue CY, Yang J (2013) Surface microstructures and epoxy bonded shear strength of Ti6Al4V alloy anodized at various temperatures. Compos Sci Technol 82:15–22. https://doi.org/10.1016/j.compscitech.2013.04.007
20. Marín-Sánchez M, Conde A, García-Rubio M, Lavia A, García I (2016) Durability of titanium adhesive bonds with surface pretreatments based on alkaline anodisation. Int J Adhes Adhes 70:225–233. https://doi.org/10.1016/j.ijadhadh.2016.07.001
21. Wu S (1973) Polar and nonpolar interactions in adhesion. J Adhes 5:39–55. https://doi.org/10.1080/00218467308078437
22. Wu S (1971) Calculation of interfacial tension in polymer systems. J Polym Sci Part C Polym Symp 34:19–30. https://doi.org/10.1002/polc.5070340105
23. Sakai H, Fujii T (1999) The dependence of the apparent contact angles on gravity. J Colloid Interface Sci 210:152–156. https://doi.org/10.1006/jcis.1998.5940
24. Extrand CW, In Moon S (2010) When sessile drops are no longer small: transitions from spherical to fully flattened. Langmuir 26:11815–11822. https://doi.org/10.1021/la1005133
25. Vesel A, Mozetic M (2017) New developments in surface functionalization of polymers using controlled plasma treatments. J Phys D Appl Phys 50:293001. https://doi.org/10.1088/1361-6463/aa748a

26. Moulder JF, Stickle WF, Sobol PE, Bomben KD (1992) Handbook of X-ray photoelectron spectroscopy. https://doi.org/10.1002/sia.740030412
27. Lee H, Ohsawa I, Takahashi J (2015) Effect of plasma surface treatment of recycled carbon fiber on carbon fiber-reinforced plastics (CFRP) interfacial properties. Appl Surf Sci 328:241–246. https://doi.org/10.1016/j.apsusc.2014.12.012
28. Li S, Sun T, Liu C, Yang W, Tang Q (2018) A study of laser surface treatment in bonded repair of composite aircraft structures. R Soc Open Sci 5. https://doi.org/10.1098/rsos.171272
29. Mittal K (2015) Advances in contact angle, wettability and adhesion, vol 2. https://doi.org/10.1002/9781119117018
30. Baldan A (2012) Adhesion phenomena in bonded joints. Int J Adhes Adhes 38:95–116. https://doi.org/10.1016/j.ijadhadh.2012.04.007
31. Maeva E, Severina I, Bondarenko S, Chapman G, O'neill B, Severin F et al (2004) Acoustical methods for the investigation of adhesively bonded structures: a review. Can J Phys 82:981–1025
32. Pizzorni M, Gambaro C, Lertora E, Mandolfino C (2018) Effect of process gases in vacuum plasma treatment on adhesion properties of titanium alloy substrates. Int J Adhes Adhes 86:113–122. https://doi.org/10.1016/j.ijadhadh.2018.07.007